Original Article

MOLECULAR METABOLISM

Neuraminidase 1 activates insulin receptor and reverses insulin resistance in obese mice

Anne Fougerat [1], Xuefang Pan [1], Victoria Smutova [1], Nikolaus Heveker [1], Christopher W. Cairo [2], Tarik Issad [3], Bruno Larrivée [4], Jeffrey A. Medin [5], Alexey V. Pshezhetsky [1,6,*]

ABSTRACT

Objectives: Neuraminidase 1 (NEU1) cleaves terminal sialic acids of glycoconjugates during lysosomal catabolism. It also modulates the structure and activity of cellular surface receptors affecting diverse pathways. Previously we demonstrated that NEU1 activates the insulin receptor (IR) and that NEU1-deficient *CathA*$^{S190A\text{-}Neo}$ mice (hypomorph of the NEU1 activator protein, cathepsin A/CathA) on a high-fat diet (HFD) develop hyperglycaemia and insulin resistance faster than wild-type animals. The major objective of the current work was to reveal the molecular mechanism by which NEU1 desialylation activates the IR and to test if increase of NEU1 activity in insulin target tissues reverses insulin resistance and glucose intolerance.

Methods: To test if desialylation causes a conformational change in the IR dimer we measured interaction between the receptor subunits by Bioluminescence Resonance Energy Transfer in the HEK293T cells either overexpressing NEU1 or treated with the NEU1 inhibitor. The influence of NEU1 overexpression on insulin resistance was studied *in vitro* in palmitate-treated HepG2 cells transduced with NEU1-expressing lentivirus and *in vivo* in C57Bl6 mice treated with HFD and either pharmacological inducer of NEU1, Ambroxol or NEU1-expressing adenovirus. NEU1-deficient *CathA*$^{S190A\text{-}Neo}$ mice were used as a control.

Results: By desialylation of IR, NEU1 induced formation of its active dimer leading to insulin signaling. Overexpression of NEU1 in palmitate-treated HepG2 cells restored insulin signaling, suggesting that increased NEU1 levels may reverse insulin resistance. Five-day treatment of glycemic C57Bl6 mice receiving HFD with the activator of the lysosomal gene network, Ambroxol, increased NEU1 expression and activity in muscle tissue, normalized fasting glucose levels, and improved physiological and molecular responses to glucose and insulin. Ambroxol did not improve insulin sensitivity in obese insulin-resistant *CathA*$^{S190A\text{-}Neo}$ mice indicating that the Ambroxol effect is mediated through NEU1 induction. Sustained increase of liver NEU1 activity through adenovirus-based gene transfer failed to attenuate insulin resistance most probably due to negative feedback regulation of IR expression.

Conclusion: Together our results demonstrate that increase of NEU1 activity in insulin target tissues reverses insulin resistance and glucose intolerance suggesting that a pharmacological modulation of NEU1 activity may be potentially explored for restoring insulin sensitivity and resolving hyperglycemia associated with T2DM.

Keywords Neuraminidase 1; Ambroxol; Insulin resistance; Insulin signaling

1. INTRODUCTION

Type 2 diabetes mellitus (T2DM) is a chronic metabolic disorder characterized by hyperglycemia resulting from the combination of resistance to insulin action and inadequate insulin secretion. The prevalence of T2DM is increasing at an alarming rate, reflecting changes in the lifestyle and making the disease one of the main public healthcare problems worldwide [1,2]. Insulin resistance is a key pathogenic feature of T2DM eventually leading to compensatory increase of insulin secretion and β-cell hypertrophy [3]. Insulin resistant condition in T2DM is caused by defects in one or several levels of the insulin-signaling cascade, which regulates glucose, lipid, and energy homeostasis, predominantly *via* action on insulin-responsive tissues (e.g. liver, skeletal muscle and white adipose tissue).

The insulin receptor (IR) plays a major role in transduction of the insulin signal across the plasma membrane. Insulin binding to the IR triggers a

[1]CHU Sainte-Justine Research Centre, Departments of Biochemistry and Pediatrics, University of Montreal, Montreal, Canada [2]Alberta Glycomics Centre and Department of Chemistry, University of Alberta, Edmonton, Alberta, T6G 2G2, Canada [3]INSERM U1016, CNRS UMR8104, Université Paris Descartes Sorbonne Paris Cité, Institut Cochin, Paris, France [4]Maisonneuve-Rosemont Hospital Research Centre, Montreal, Canada [5]Medical College of Wisconsin, Milwaukee, USA [6]Department of Anatomy and Cell Biology, McGill University, Montreal, Canada

*Corresponding author. CHU Sainte-Justine Research center, 3175 Côte Ste-Catherine, Montreal, Qc, H3T 1C5, Canada. Fax: +514 345 4766. E-mail: alexei.pchejetski@umontreal.ca (A.V. Pshezhetsky).

Abbreviations: NEU1, neuraminidase 1; HFD, high-fat diet; IR, insulin receptor; T2DM, type 2 diabetes mellitus; AV, adenovirus; LV, lentivrus; BRET, bioluminescence resonance energy transfer; DANA, 2,3-dehydro-2-deoxy-N-acetylneuraminic acid; IGTT, intraperitoneal glucose tolerance test; ITT, insulin tolerance test; PA, palmitate, Ambroxol, trans-4-(2-Amino-3,5-dibromobenzylamino)cyclohexanol; TFEB, transcription factor EB; PNA, peanut agglutinin

Received December 20, 2017 • Revision received March 23, 2018 • Accepted March 30, 2018 • Available online 21 April 2018

https://doi.org/10.1016/j.molmet.2018.03.017

signaling cascade that involves phosphorylation and activation of multiple proteins leading to glucose uptake, regulation of gene expression, synthesis of triglycerides in adipocytes and of glycogen in the liver [4]. Human IR is heavily glycosylated in the β-chain with multiple species of complex N-linked glycans which are important for proper folding, maturation, targeting and activity of the receptor and consequently for insulin signal transduction [5,6]. In particular, aberrantly glycosylated IR does not form dimers nor undergoes insulin-sensitive autophosphorylation [7], while receptors lacking specific glycan chains showed a constitutive tyrosine kinase activity [8]. These signaling cascades are intensively studied in a search for novel therapeutic targets for T2DM and its complications.

Recently, there has been a growing interest in the potential role of neuraminidases (sialidases) in the regulation of metabolic pathways [9–14], including glucose homeostasis [15–17]. Neuraminidases catalyze the removal of sialic acid residues from glycan chains of glycoproteins, oligosaccharides and sialylated glycolipids, and together with sialyltransferases modulate molecular and cellular recognition events (reviewed in [18]). Emerging data have demonstrated that mammalian neuraminidase 1 (NEU1) modulates cellular receptors involved in diverse signaling pathways. NEU1 cleaves sialic acids on the glycan chains of receptors, which changes their structure and activity resulting in either activation or inhibition of the receptor [19,20]. Recent data from our lab and others demonstrated that IR is one of the receptors modulated by NEU1 [16,17,21,22]. We also showed that genetically-modified CathA$^{S190A\text{-}Neo}$ mice (a hypomorph of the NEU1 activator protein, cathepsin A/CathA) that have 10% of normal NEU1 activity in their tissues develop glucose intolerance and insulin resistance after exposure to high-fat diet (HFD) more rapidly than their wild-type counterparts and show impaired insulin signaling in their tissues [16]. At a molecular level, insulin binding to IR rapidly induces its interaction with NEU1, which hydrolyzes sialic acids in the glycan chains of the receptor and, consequently, induces its activation [16]. This study led us to hypothesize that increase of NEU1 activity in insulin target tissues has an opposite protective effect and reverses insulin resistance and glucose intolerance in the mice with HFD-induced obesity.

In our current work, we reveal the molecular mechanism by which NEU1 desialylation activates the IR. We also show that acute pharmacological increase of NEU1 activity in insulin target tissues may reverse insulin resistance and glucose intolerance induced in mice by obesity. Thus, selective targeting of NEU1 may represent a novel therapeutic strategy for restoring insulin sensitivity and resolving hyperglycemia associated with T2DM.

2. MATERIAL AND METHODS

2.1. Construction of recombinant vectors

NEU1 cDNA was PCR-modified to remove the stop codon and inserted into the pEGFP-N1 plasmid between the XhoI and SmaI restriction sites in the multiple cloning site (MCS) region. The CathA-IRES-NEU1 and CathA-IRES-NEU1-GFP biscistronic recombinant plasmids were constructed by removing the hIL12 and CD19tmpk from pDy.hIL12.IRES.CD19tmpk. WS vector [23] and replaced respectively by CathA and NEU1 (NEU1-GFP) cDNA. The NEU1 and NEU1-GFP cDNA were PCR-modified and inserted in the MCS of the pDy.hIL12.IRES.CD19tmpk. WS between the XbaI and BamHI sites. The CathA cDNA was PCR-modified and inserted into the MCS of pDy.hIL12.IRES.NEU1-GFP and pDy.hIL12.IRES.NEU1 between the EcoRI and AscI sites. All constructs were verified by PCR, enzymatic digestions and DNA sequencing. The final CathA-IRES-NEU1 and CathA-IRES-NEU1-GFP constructs were assessed for sialidase activity in transfected HEK293T cells.

2.2. CathA-IRES-NEU1-GFP adenovirus production and titration

For the production of adenovirus, the CathA-IRES-NEU1-GFP cDNA was modified by PCR and cloned into the pENTR1A plasmid between the SalI and NotI restriction sites. Thereafter, the CathA-IRES-NEU1-GFP insert was transferred into pAd/CMV/V5/DEST plasmid using the Gateway System (Invitrogen). To make adenovirus, HEK293A cells were transfected with the Pac1-linearized adenoviral construct using Lipofectamine 2000 (Invitrogen). After 14–21 days, cells were harvested and adenovirus was released from the cells by four freeze–thaw cycles [24]. Adenovirus was further amplified by three rounds of re-infection of HEK293A cells. The titer of the virus was determined by measuring GFP-positive cells using flow cytometry 48 h after infection of HEK293A cells with various dilutions of adenovirus. For *in vivo* experiments, mice were injected intravenously with 10^9 TU/200 μl/mouse 1 day after the start of HFD and sacrificed after 20 weeks.

2.3. CathA-IRES-NEU1-GFP lentivirus production and titration

The CathA-IRES-NEU1-GFP biscistronic HIV-1-based recombinant vesicular stomatitis virus glycoprotein-pseudotyped (VSVg) LV and control NEU1-GFP LV were generated by transient transfections of HEK293T cells by LV plasmid construct, packaging plasmid pCMVDR8.91 and the VSV-g envelope-coding plasmid pMD.G as described previously [25]. The titer of concentrated LV was measured on HeLa cells (ATCC) by flow cytometric analysis for GFP expression, 72 h after infection. LV titers were 1.4×10^8 TU/ml for CathA-IRES-NEU1-GFP LV and 8.3×10^8 TU/ml for control NEU1-GFP LV.

2.4. Analysis of interaction between NEU1 and IR by BRET

HEK293T cells seeded at a density of 5×10^5 cells per well in 6-well plates were transiently transfected using polyethylenimine with 0.5 μg IR-Rluc and 2 μg IR-YFP [26,27] plasmids with or without CathA-IRES-NEU1 plasmid. The total amount of DNA was brought to 4.5 μg using empty vectors. After 24 h, transfected cells were transferred into 96-well microplates (white culturPlate-96; Packard, Meriden, CT) at a density of 30,000 cells per well. On the following day (48 h after transfection) cells were washed with phosphate-buffered saline (PBS), then incubated in PBS at room temperature for 10 min with the luciferase substrate cœlenterazine H at a final concentration of 5 μM. Then insulin (Sigma), on 50 nM concentration was added and light-emission acquisition started immediately. The interaction was monitored for at least 30 min using the Mithras LB 940. To measure the effect of the NEU1 inhibitor DANA (2,3-dehydro-2-deoxy-N-acetylneuraminic acid) it was added to the cells in 1 mM concentration (5 K_I) 90 min before BRET experiments. The results were expressed as delta BRET by subtracting the BRET signal for the basal condition (IR-Rluc + IR-YFP without insulin) from the mean values of the BRET signal recorded between 5 and 15 min for each condition.

2.5. Sialidase activity assay

Sialidase activity in cell and tissue homogenates was assayed using the synthetic fluorogenic substrate 2-(4-methylumbelliferyl)-D-*N*-acetylneuraminic acid (4MU-NeuAc; Sigma) as previously described [16]. NEU1 sialidase activity was assayed in the presence of 100 μM C-9-(4-biphenyl-triazolyl)-DANA (C9-4BPT-DANA) that causes complete inhibition of NEU3 and NEU4 isoenzymes [28]. Protein concentration was measured using a protein assay kit (Bio-Rad).

2.6. Analysis of insulin signaling in insulin resistant HepG2 cells by western blot

HepG2 (liver hepatocellular carcinoma) cells were cultured in DMEM supplemented with 10% FBS, 1% streptomycin-penicillin at 37 °C in a humidified 5% CO_2 atmosphere. To overexpress NEU1, cells were transduced with CathA-IRES-NEU1-GFP or control NEU1-GFP LV at 10 MOI in the presence of polybrene (8 μg/ml).

Five days after transduction, a portion of the cells was harvested to verify NEU1 expression by measuring acidic sialidase activity in the cell lysate. The remaining cells were deprived of FBS for 16 h and conditioned for 24 h with palmitate-containing medium to induce insulin resistance [29]. Then the cells were washed twice with ice-cold PBS and lysed with RIPA buffer (50 mM Tris HCl, pH 7.4, 150 mM NaCl, 2 mM EDTA, 0.1% SDS, 1 mM PMSF, 1% NP40, 0.25% sodium deoxycholate, proteinase and phosphatase inhibitors (Roche)). The protein concentration in each lysate was measured using Bio-Rad Protein Assay Reagent (Bio-Rad).

Proteins were separated by SDS-polyacrylamide gel electrophoresis and transferred onto nitrocellulose membrane. Immunodetection was performed as previously described [16] using the relevant primary antibody: anti-pSer473Akt, Cat# 9271; anti-Akt, Cat# 9272; anti-insulin receptor β-chain, Cat# 3020; anti-pTyr1162/1163 insulin receptor, Cat# 3026S; anti-IRS1, Cat# 2390; anti-pSer307IRS1, Cat# 2381; anti-phosphorylated p38MAPK, Cat# 9211; anti-p38MAPK, Cat# 9212 (all Cell Signaling, dilutions recommended by the manufacturer) overnight at 4 °C. The total and phosphorylated proteins were analyzed on different blots from SDS PAGE gels ran in parallel in the same tank. Signals were acquired using AFP Mini Medical Series 90 imager and quantified using ImageJ software. Signal intensities obtained with phospho-specific antibodies were normalized for those obtained with antibodies against total proteins.

2.7. Analysis of IR sialylation by lectin blot

IR was partially purified from Triton-X 100 extracts of liver tissue from Ambroxol-treated and saline-treated control mice using WGA-agarose (MJSBioLynx Inc.) as previously described [30], resolved by SDS-PAGE and transferred to nitrocellulose membrane. Blots were stained with biotinylated PNA lectin (Vector Labs, 1:2000 dilution), followed by HRP-conjugated streptavidin and an enhanced chemiluminescence kit. Total amount of receptor was measured by Western blot with anti-insulin receptor β-chain antibodies (Cell Signaling).

2.8. Animal studies

Approval for the animal care and the use in the experiments was granted by the Animal Care and Use Committee of CHU Ste-Justine. C57BL/6J WT mice and previously described $CathA^{S190A-Neo}$ mice with ~90% reduction of NEU1 activity [31] were maintained on a 12 h dark/light cycle. Four-month-old (~25 g BW) male mice received *ad libitum* water and either normal diet (5% fat, 57% carbohydrate) or HFD (35% fat, 36% carbohydrate, Bio-Serv). Body weight and total food consumption were measured. In the first study, after 7 weeks on HFD, NEU1 activity was induced pharmacologically in mice by intraperitoneal injection of Ambroxol hydrochloride (Sigma) at the dose of 60 mg/kg body weight/mouse for 5 consecutive days. In the second study, 4-month-old mice were fed with HFD and injected one day later through the tail vein with adenovirus expressing CathA-IRES-NEU1-GFP or control NEU1-GFP at a dose of 10^9 TU/mouse in 0.2 ml of saline. These mice were fed with a HFD continuously before sacrifice 20 weeks later. Intraperitoneal Glucose Tolerance Test (IGTT) and Insulin Tolerance Test (ITT) were conducted as described [16].

2.9. Analysis of insulin signaling in animal tissues by western blot

Mice fasted for 4 h received intraperitoneal injections of insulin (Humulin R; Eli Lilly) at 1 unit/kg BW, and were sacrificed 20 min later by cervical dislocation. Saline-injected animals were used as a 0-min time point. Tissues were immediately removed and homogenized in RIPA buffer by sonication. Particulate was removed by 30 min centrifugation at 13,000 g. Western blots were performed as described for HepG2 cells.

2.10. Quantification of cytokines in mouse tissues by real time quantitative PCR

Total RNA was extracted from mouse tissues using the Trizol reagent (Invitrogen); phase separation was performed with chloroform and RNA precipitation with isopropanol. RNA concentrations were determined by measuring UV absorbance. One microgram of total RNA was used for cDNA synthesis with random primers and SuperScript III reverse transcriptase (Invitrogen). The cDNA was amplified by quantitative real time-PCR with SYBR Green (Roche). All real-time PCR reactions were performed on a Stratagene Mx3000P QPCR System as described before [32]. The values were normalized to the relative amounts of Rpl32.

2.11. Analysis of plasma lipids

LDL, cholesterol, triglycerides, and HDL levels in the mouse plasma were measured in CHU Sainte-Justine central biochemistry laboratory using the glycerol phosphate oxidase and cholesterol esterase methods as previously described [33,34].

2.12. Statistical analysis

Statistical analysis has been performed by unpaired 2-tailed Student's *t* or ANOVA tests using Prism GraphPad software to compare differences between groups. A *P*-value of 0.05 was considered significant.

3. RESULTS

3.1. NEU1 induces formation of IR active dimer

Previously we demonstrated that activation of the IR occurs within 30 s after induction of its interaction with NEU1 suggesting that it is caused by a direct action of NEU1 on the receptor [16]. To test if the activation results from a conformational change in the IR dimer caused by desialylation we used Bioluminescence Resonance Energy Transfer (BRET) in a chimeric receptor with one β-subunit fused to Renilla luciferase (Rluc) and another, to the yellow fluorescent protein (YFP) [27]. The molecular interactions between the IR subunits were studied in the presence or in the absence of NEU1, the NEU1 inhibitor DANA and insulin. If desialylation of IR by NEU1 induces favorable changes in the conformation of the IR dimer and activates the receptor it would be detected by the increase in the resonance energy transfer (BRET signal) between Rluc and YFP (Figure 1A).

As expected, our experiments showed that 50-nM insulin induces the BRET signal between the IR subunits reflecting a conformational change occurring during the activation of the receptor (Figure 1B). Importantly, the increase of BRET intensity was blocked by pre-incubation of cells with DANA suggesting that inhibition of NEU1 prevents receptor from obtaining the active conformation. In contrast, transfection of cells with NEU1/CathA-encoding plasmid that increased sialidase activity ~50-fold (Supplementary Fig. 1) significantly induced the BRET signal. Similarly, to what was observed in untransfected cells, the increase of BRET signal was inhibited by DANA (Figure 1B).

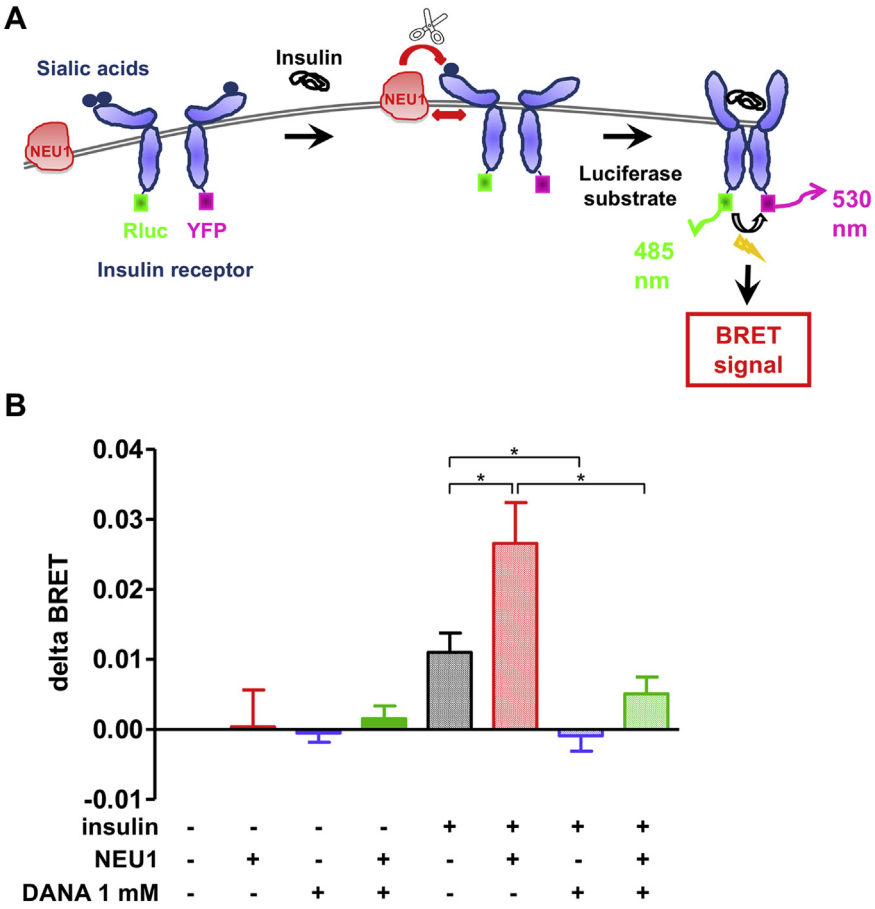

Figure 1: Desialylation of IR by NEU1 induces the active conformation of IR dimer. (**A**) Schematic representation of the analysis of NEU1-induced conformational changes in the chimeric IR dimer using the BRET assay. Rluc fused to the C-terminus of one IR β-subunit converts the luciferase substrate coelenterazine causing light emission at 480 nm. If IR desialylation by NEU1 causes a conformational change that brings together (at a distance <100 Å) the two β-subunits of the receptor and results in a transfer of energy between Rluc and EYFP fused to the other IR β-subunit and an increased BRET signal at 530 nm. (**B**) BRET assay in HEK293T cells co-transfected with IR-YFP and IR-Rluc with or without NEU1-encoding plasmid, pre-treated or not with 1 mM DANA for 1.5 h. Transfection with NEU1 plasmid increases and pre-treatment with DANA inhibits the delta BRET signal. In all panels, the BRET signal was calculated as the ratio of light intensity emitted by Rluc (530 nm) and YFP (480 nm). Data represent the mean ± s.e.m. of at least three independent experiments. * Statistically significant difference as measured by *t*-test ($P < 0.05$).

3.2. Overexpression of NEU1 in palmitate-treated HepG2 cells restores insulin signaling

We further tested if NEU1 overexpression could induce IR signaling and reverse lipid-induced insulin resistance in cultured cells. HepG2 cells were transduced with a lentivirus (LV) engineering expression of GFP or NEU1-GFP. After 5 days, when sialidase activity in NEU1-GFP-transduced cells increased ~2.5 fold as compared with control GFP-transduced cells (Figure 2A), the cells were treated for 24 h with 0.25 mM palmitate (PA)-BSA or BSA only in a serum-free medium to induce insulin resistance. After 20 min stimulation of the cells with 100 nM insulin, phosphorylation of Akt and a marker of insulin resistance, stress-sensitive serine/threonine p38 MAP kinase was evaluated by western blots. As expected treatment of HepG2 cells with palmitate blocks phosphorylation of Akt in response to insulin and induces constitutive phosphorylation of p38 MAP kinase associated with glucolipotoxicity-induced apoptosis and insulin resistance [35] (Figure 2B). In contrast, the cells overexpressing NEU1 despite showing substantial p38 phosphorylation retain the ability to phosphorylate Akt in response to insulin stimulation (Figure 2B).

3.3. Ambroxol reverses insulin resistance in glycemic C57Bl6 mice by increasing the *Neu1* gene expression

We further tested if increased levels of NEU1 activity can also induce IR signaling *in vivo*, reversing insulin resistance in mice with HFD-induced obesity. We used a pharmacological approach where we induced NEU1 by treating mice with Ambroxol [trans-4-(2-Amino-3,5-dibromobenzylamino)cyclohexanol] hydrocholoride, which previously has been shown to increase the *Neu1* gene expression at least 3-fold, presumably by activating TFEB transcription factor [36]. In our preliminary experiments treatment of cultured human fibroblasts with 60-μM Ambroxol for 3 days increased acidic sialidase activity ~3-fold (Supplementary Fig. 2). After demonstrating that Ambroxol induces NEU1 activity we studied the effect of the drug on glucose metabolism and insulin signaling in male C57Bl6 mice. Starting from the age of 4 months all mice received a HFD to induce obesity and insulin resistance. Intraperitoneal Glucose Tolerance Test (IGTT) was conducted at 0, 5 and 7 weeks and insulin sensitivity was measured by Insulin Tolerance Test (ITT) at 1, 6 and 8 weeks after the start of HFD. At 7 weeks on HFD when mice demonstrated hyperglycemia in IGTT

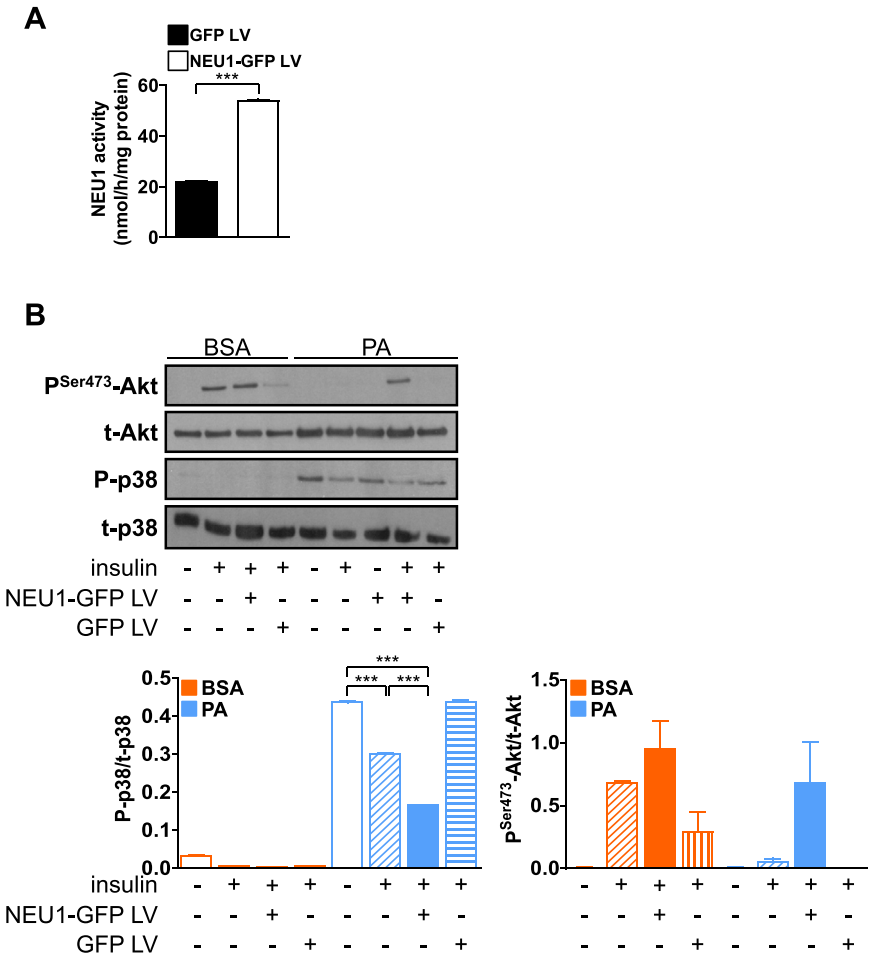

Figure 2: NEU1 overexpression through LV based-gene transfer reverses palmitate-induced insulin resistance in HepG2 cells. HepG2 cells were transduced with a lentivirus (LV) expressing GFP or NEU1-GFP at a multiplicity of infection of 10 for 5 days and treated with palmitate (PA, 0.25 mM)-BSA or BSA only in serum-free medium for the last 24 h. (**A**) Neuraminidase activity in cell homogenates was measured using the fluorigenic substrate 4MU-NeuAc. (**B**) After 20 min stimulation of the cells with 100 nM insulin, phosphorylation of Akt and p38 in cell lysates was studied by western blot. The panel shows the representative image and bar graph, mean ± s.e.m from two independent experiments. *** Statistically significant difference as measured by *t*-test ($P < 0.001$).

(Supplementary Fig. 3) they were separated into 2 groups with equal average IGTT profile, weight gain rate, fat/lean body mass assessed by dual energy X-ray absorptiometry and daily food intake. In the first group mice were injected intraperitoneally with Ambroxol at 60 mg/kg body weight/day for 5 consecutive days. Mice in the second group received daily intraperitoneal injections of saline. On the 5th day of treatment the level of fasted glucose was significantly lower in Ambroxol-treated than in saline-treated group (Figure 3A) and Ambroxol treated mice showed better glucose tolerance in IGTT (Figure 3B). On the 8th day we conducted ITT in which mice fasted for 4 h received intraperitoneal injections of insulin (1 unit/kg BW) and blood glucose was measured 10 and 20 min after injections. We found that Ambroxol-treated mice showed significantly improved blood glucose response to insulin as compared to saline-treated group (Figure 3C). Immediately after ITT mice were sacrificed and phosphorylation of IR and Akt in the insulin target tissues was studied by western blots. While intraperitoneal injections of insulin significantly induce phosphorylation of IR and Akt in control mice kept on normal diet (results not shown), after 8 weeks on HFD, the changes in phosphorylation of both proteins after insulin treatment were not significant (Figure 4A). In contrast, after 8 days of treatment with Ambroxol, both Akt and IR were efficiently phosphorylated (Figure 4A).

Tissues from Ambroxol-treated and control saline-treated mice were harvested to study expression and activity of NEU1 and sialylation of IR. *Neu1* mRNA level measured by quantitative RT-PCR was significantly increased in the muscle tissues of Ambroxol-treated mice (Figure 5A) as well as the level of NEU1 activity measured with fluorigenic substrate 4MU-NeuAc at acidic pH 4.2 (to discriminate it from NEU2 that has a neutral pH-optimum) and in the presence of 100 μM C-9-(4-biphenyl-triazolyl)-DANA (C9-4BPT-DANA) that causes complete inhibition of NEU3 and NEU4 isoenzymes (Figure 5B) [28]. The sialylation level of IR purified from liver tissue Triton X-100 extract using WGA agarose [30] was studied by blotting with peanut agglutinin (PNA) specific to carbohydrate sequence Gal-β(1−3)-GalNAc (Figure 5C). Our results show that in Ambroxol-treated mice staining of IR with PNA increased confirming removal of the terminal Sia residues form the glycan chains. The sensitivity of lectin blotting was not sufficient to study IR sialylation in the muscle extract.

Since Ambroxol induces the expression of multiple genes besides NEU1 which may potentially affect insulin-signaling pathway, we

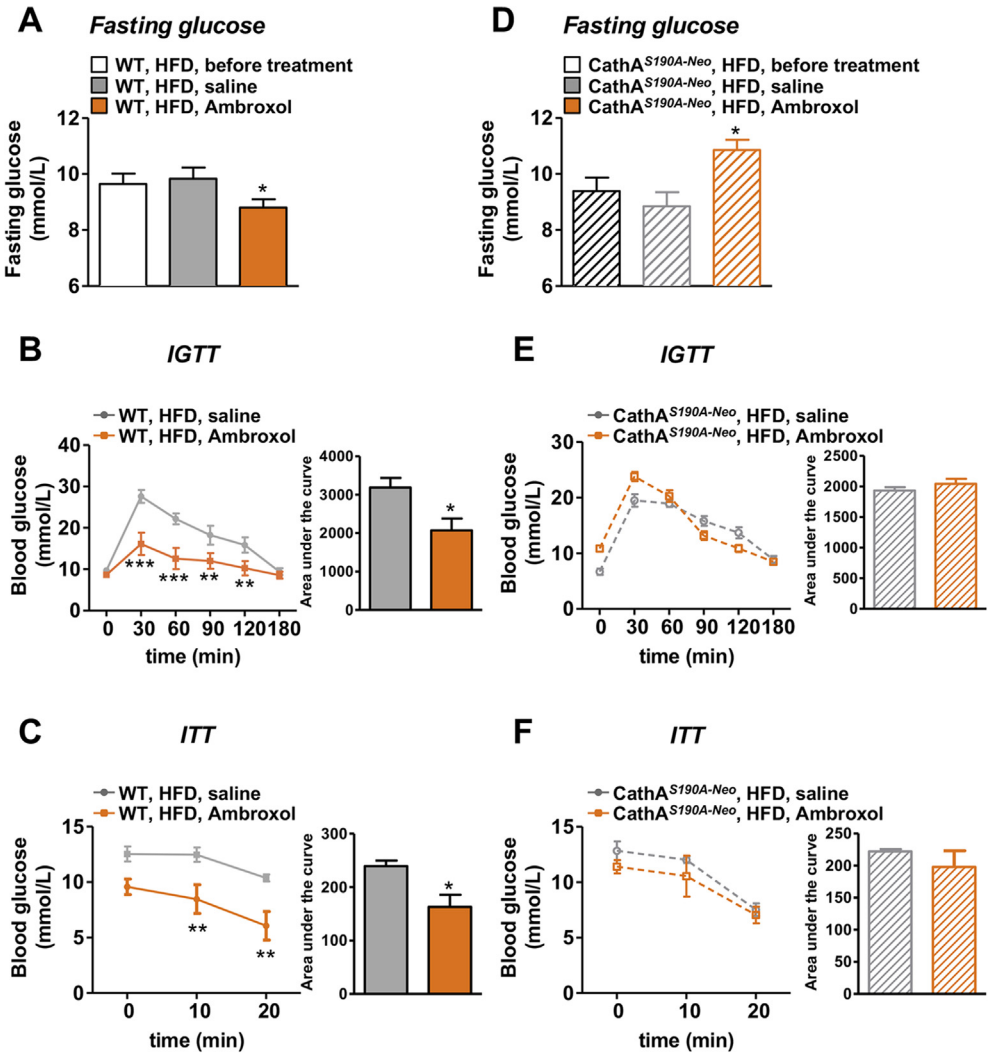

Figure 3: Acute pharmacological induction of NEU1 by Ambroxol improves glucose tolerance and insulin resistance in mice exposed to HFD. Four-month-old C57Bl/6 WT mice (**A, B, C**) or CathA$^{S190A-Neo}$ mice (**D, E, F**) exposed to HFD for 7 weeks were injected intraperitoneally with Ambroxol hydrochloride in saline at the dose of 60 mg/kg body weight (BW) (n = 6 in each genotype) or saline only (n = 5 in each genotype) for 8 consecutive days. (**A, D**) Blood glucose level was measured after 5 days of treatment and a 12 h fasting period. (**B, E**) Intraperitoneal glucose tolerance test, IGTT (2 g/kg body weight, intraperitoneal injection of glucose) and corresponding area under the curve (AUC) of blood glucose levels after 5 days of treatment. (**C, F**) Insulin tolerance test, ITT (1 U/kg BW, intraperitoneal injection with insulin) and corresponding area under the curve (AUC) of blood glucose levels after 8 days of treatment. Data are shown as means ± s.e.m. Significant (*$P < 0.05$, **$P < 0.01$, ***$P < 0.001$) difference was detected with saline group. Data were analyzed using two-way repeated measures ANOVA, Bonferroni posttest (panels **B, C, E, F**) or *t*-test (panels **A, B**, areas under the curves in panels **B, C, E, F**). The graphs show data of one of 2 independent studies performed 3 months apart and yielding similar results.

further tested if the drug had similar effect in NEU1-deficient CathA$^{S190A-Neo}$ mice. In agreement with our previous data [16] already after 4 weeks of HFD CathA$^{S190A-Neo}$ mice have developed insulin resistance and demonstrated increased fasting glucose and glycemia in IGTT. In contrast with the WT group, there was no improvement in fasting glucose, glucose tolerance and glucose response to insulin in Ambroxol-treated as compared with saline-treated CathA$^{S190A-Neo}$ mice (Figure 3D,E,F). Furthermore, insulin signaling study in muscle tissue demonstrated that although CathA$^{S190A-Neo}$ mice still showed some insulin-induced Akt phosphorylation, Ambroxol injections had no influence on the level of Akt or IR phosphorylation (Figure 4B). Altogether, these results were consistent with the suggestion that Ambroxol in insulin-resistant mice is acting by increasing NEU1 levels.

3.4. Sustained increase of liver NEU1 activity through adenovirus-based gene transfer does not attenuate insulin resistance in mice receiving HFD

We further tested whether a long-term induction of NEU1 would protect mice from HFD-induced insulin resistance. To achieve lasting supra-physiological levels of NEU1 activity we used a recombinant adenovirus (AV)-based gene transfer approach. AV typically allows ~100-fold increased expression of enzymes in mouse liver tissues [37,38] for a period of up to 3 months [39]. The NEU1 cDNA tagged at the C-terminus with GFP and the cDNA of its activator protein, CathA, were sub-cloned into biscistronic AV-based recombinant vector and the virus was generated and tested in cultured HepG2 cells, transduced at MOI of 10 and 50. At day 3 post-transduction with NEU1-GFP AV, ~60% of cells were expressing GFP. Sialidase activity of cells

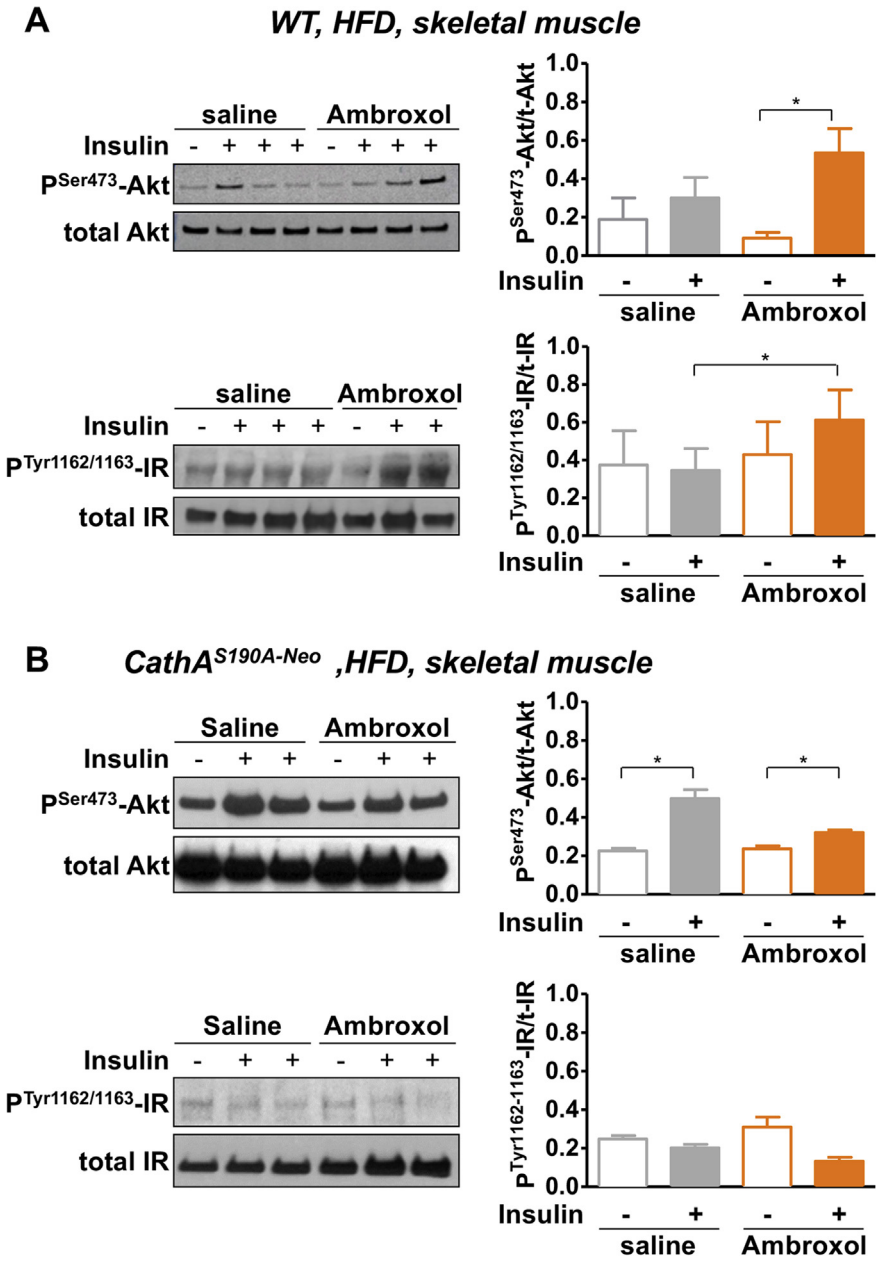

Figure 4: Acute pharmacological induction of NEU1 by Ambroxol improves insulin signaling in muscle tissues of mice exposed to HFD. Four-month-old C57Bl/6 WT mice (**A**) or NEU1-deficient CathA$^{S190A-Neo}$ mice (**B**) exposed to HFD for 7 weeks were injected intraperitoneally with Ambroxol hydrochloride in saline at the dose of 60 mg/kg BW (n = 6 in each genotype) or saline only (n = 5 in each genotype) for 8 consecutive days. Mice were then fasted for 4 h and killed 20 min after intraperitoneal injections of insulin at 1 U/kg BW or saline. Muscle homogenates were analyzed by western blots using antibodies against P^{Ser473}-Akt, Akt, P$^{Tyr1162/1163}$-IR and IR β-chain. Panels show typical results of two independent experiments representing all mice in each group. Graphs beside the panels show quantification of signal intensities using ImageJ software. Data are shown as means ± s.e.m. * Statistically significant difference as measured by *t*-test ($P < 0.05$).

transduced at MOI of 50 was increased ~16-fold (Supplementary Fig. 4). NEU1-GFP co-localized in the cells with the lysosomal and plasma membrane markers suggesting that the enzyme was correctly targeted (data not shown). Further a cohort of mice was infected by intravenous injection using 5 10^8 viral particles/animal which led to a ~3-fold increase of sialidase activity in the liver (but not in the other organs) lasting for at least 9 weeks (Supplementary Fig. 5).

Glucose metabolism and insulin signaling were studied in male 4-month-old C57Bl6 mice infected with NEU1-GFP and GFP-AV (10^9 viral particles/animal) and kept on HFD. In both groups, the weight gain and daily food intake were similar (Supplementary Fig. 6). Before HFD as well as at 4th and 8th week of HFD glucose tolerance was similar between NEU1-GFP and GFP AV infected mice group (Figure 6A,B), but to our surprise at 16th week on HFD mice infected with NEU1-GFP showed significantly higher blood glucose levels in IGTT than the control, GFP AV-infected group (Figure 6A). The ITT conducted at 16th week on HFD revealed that insulin sensitivity of the NEU1-GFP AV-infected group showed a trend for reduction as compared with the

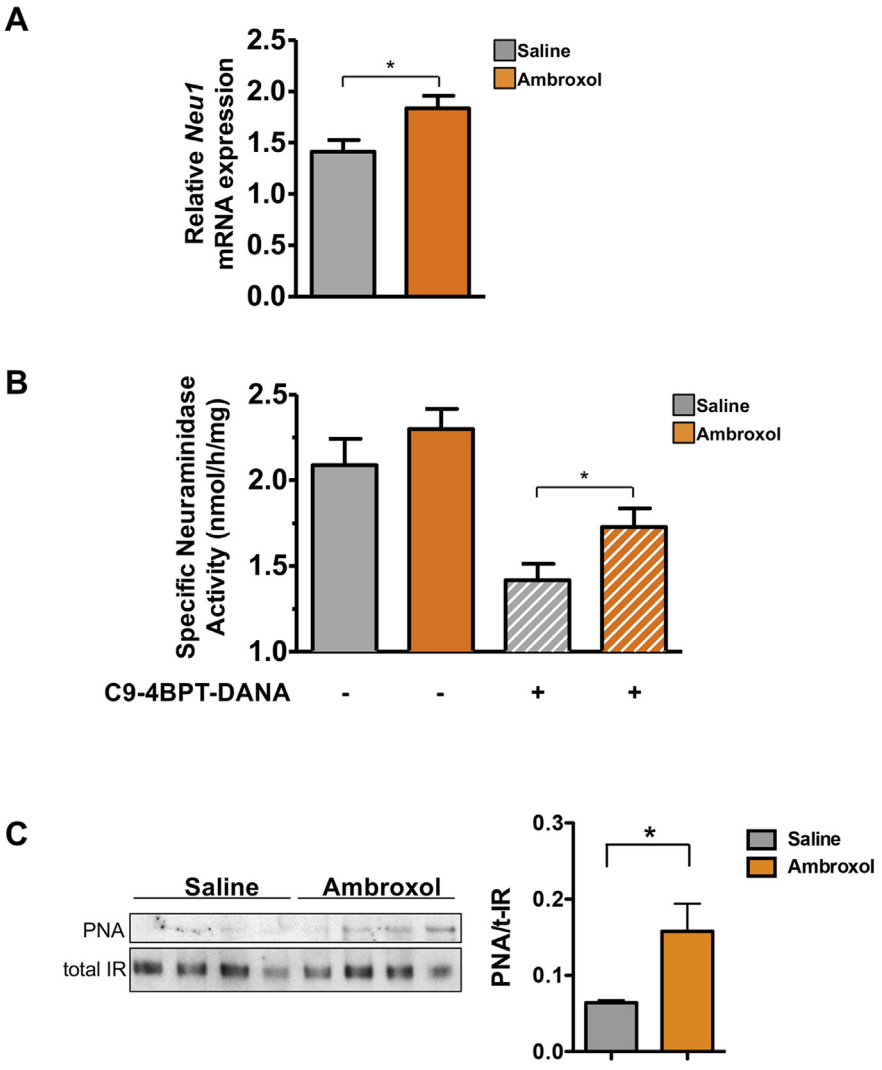

Figure 5: Ambroxol treatment induces NEU1 expression and activity and results in desialylation of IR in the muscle tissue. Four-month-old C57Bl6 mice exposed to HFD for 7 weeks were injected intraperitoneally with Ambroxol hydrochloride in saline at the dose of 60 mg/kg BW (n = 4) or saline only (n = 4) for 8 consecutive days. (**A**) Total RNA was extracted from muscle tissues, reverse-transcribed to cDNA and *Neu1* mRNA level was measured by real-time quantitative PCR. The data are normalized for the content of RLP32 mRNA and represent the mean ± s.e.m. (*$P < 0.05$ in t test). (**B**) Acidic neuraminidase activity was measured in the muscle homogenates against 4MU-NeuAc in the presence or absence of 100 μM NEU3/NEU4 inhibitor C9-4BPT-DANA. Data are shown as means ± s.e.m. * Statistically significant difference as measured by *t* test ($P < 0.05$). (**C**) Sialylation of IR purified from liver tissues of Ambroxol-treated and control saline-treated WT mice was studied by PNA lectin blotting (upper panel) or Western blotting with antibodies against the β-subunit of IR (lower panel). Bar graph shows quantification (mean values and s.e.m.) of signal intensities for lectin blots normalized for those for Western blots using ImageJ software. The panel shows the representative image from two independent experiments and bar graph, mean ± s.e.m (n = 4, *P < 0.05 in *t*-test).

GFP AV-infected group (Figure 6B). Analysis of insulin signaling in mouse liver tissues showed that in both GFP AV and NEU1-GFP AV-infected mice pIR levels were not significantly induced in response to insulin injections. In the same tissues, pAKT showed a significant increase in liver tissue of GFP AV-infected but not of NEU1-GFP-infected mice (Figure 6C). This was consistent with significantly increased p38 phosphorylation in the liver tissues of NEU1-GFP AV-infected mice indicating higher level of lipotoxicity (Figure 6D). Levels of total IR protein normalized to tubulin level were lower in NEU1-GFP AV-infected as compared with GFP AV-infected animals (Figure 6E).

We further tested levels of inflammation in the tissues of GFP AV and NEU1-GFP AV-infected mice, which could develop as a consequence of the immune response to the viral capsid proteins, GFP, or human NEU1 and/or CathA. By affecting insulin sensitivity and insulin production, inflammatory cytokines could be responsible for increased glycemia in the NEU1-GFP AV-infected group. However, expression levels of TNFα, IL-1-β and IL-6 measured by RT qPCR in the liver were similar between the groups, whereas in the white adipose tissue the cytokine expression was even higher for the control GFP AV-infected mice (Figure 7A). Besides, sialidase activity in the liver of NEU1-GFP AV-infected mice remained higher

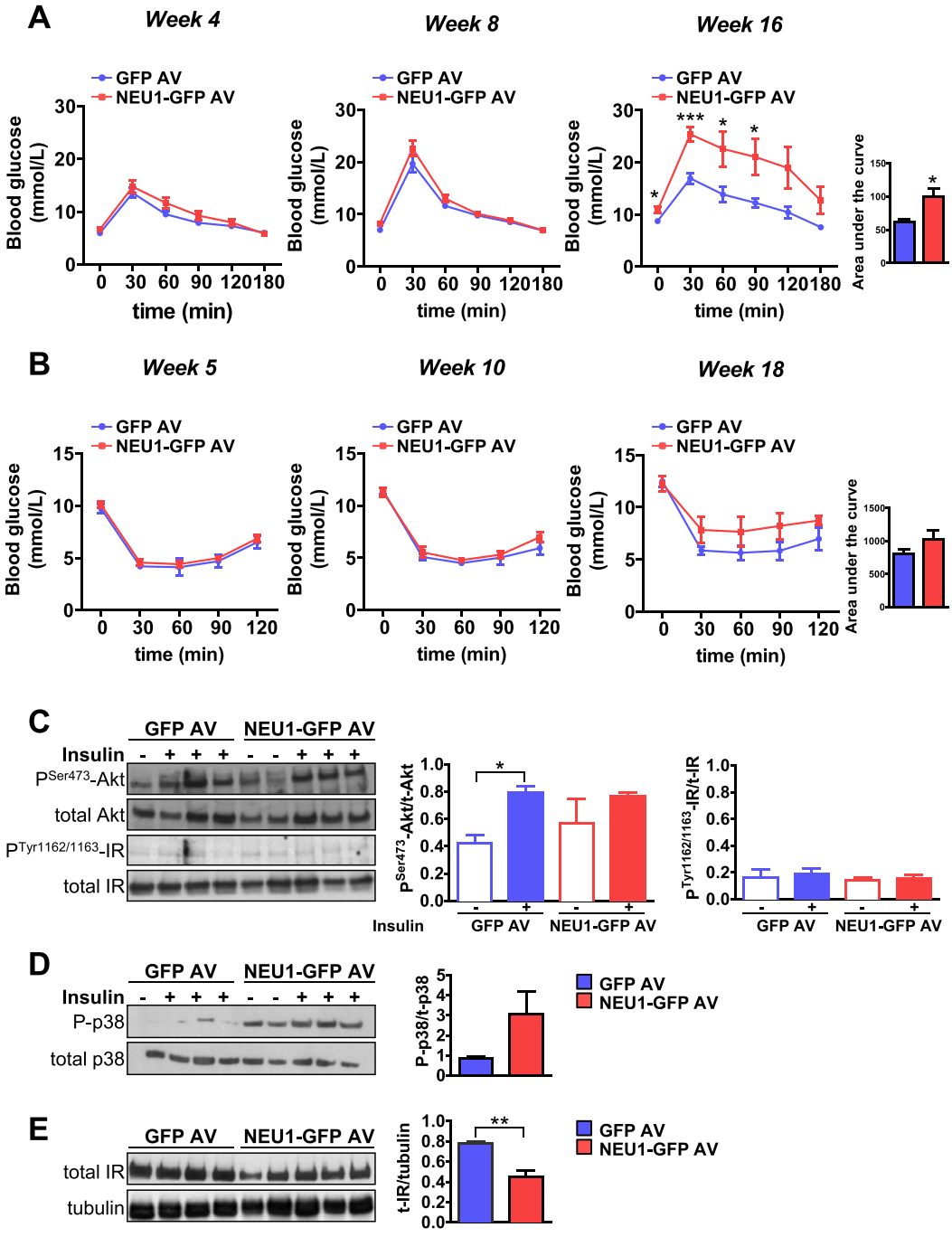

Figure 6: Long-term hepatic NEU1 overexpression through adenovirus-based gene transfer increases glucose intolerance and insulin resistance in mice exposed to HFD. Four-month-old C57Bl/6 WT mice were injected into the tail vein with NEU1-GFP adenovirus (NEU1-GFP AV) or control GFP adenovirus (GFP AV) at 10^9 pi/mouse and exposed to HFD. (**A**) IGTT (2 g/kg BW, intraperitoneal injection of glucose) and corresponding area under the curve (AUC) of blood glucose levels at 4, 8 and 16 weeks after AV injection ($n = 6–8$ in each group). (**B**) ITT (1 U/kg BW, intraperitoneal injection with insulin) and corresponding area under the curve (AUC) of blood glucose levels at 5, 10, 18 weeks after AV injection ($n = 6–8$ in each group). (**C, D** and **E**) After 20 weeks of HFD, mice were fasted for 4 h and killed 20 min after intraperitoneal injections of insulin at 1 unit/kg BW or saline. Liver homogenates were analyzed by western blots using antibodies against P^{Ser473}-Akt, Akt, $P^{Tyr1162/1163}$-IR, and IR β-chain (**C**), P-p38 and total p38 (**D**) or IR β-chain and tubulin (**E**). Panels show typical results of 2 independent experiments. Graphs beside the panels show quantification of signal intensities using ImageJ software. Data are shown as means ± s.e.m. Significant ($*P < 0.05$, $**P < 0.01$, $***P < 0.001$) difference was detected with GFP-AV group. Data were analyzed using two-way repeated measures ANOVA, Bonferroni posttest (panels **A, B**) or *t*-test (panels **C, D, E**, areas under the curves in panels **A, B**).

than that in GFP AV-infected mice even 20 weeks after injection suggesting that the immune response did not reduce NEU1 levels below the normal (Figure 7B). The levels of circulating lipids (total cholesterol, HDL, LDL and triglycerides) (Figure 7C) and the average wet weight of livers (Figure 7D) were similar between NEU1-GFP AV-infected and GFP AV-infected groups not consistent with a possibility of increased liver steatosis in NEU1-GFP AV-infected mice.

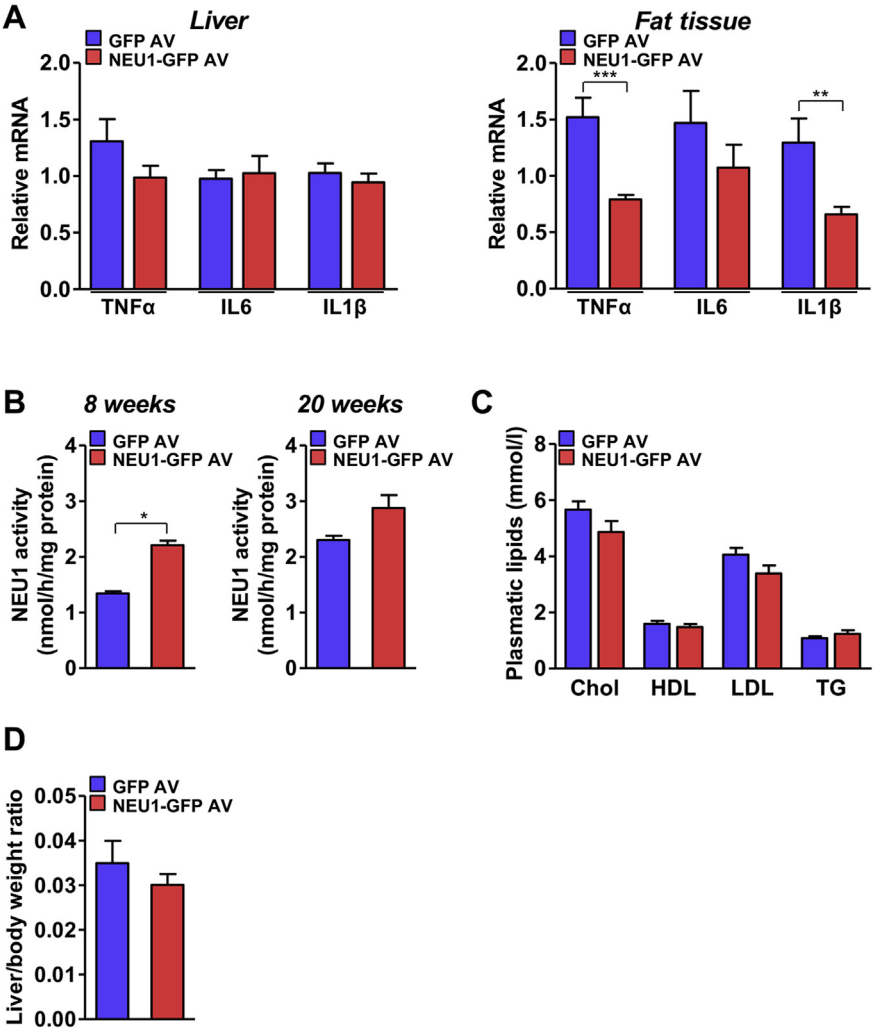

Figure 7: Mice overexpressing NEU1 in the liver do not show increased tissue inflammation, liver weight or altered lipid blood profiles. Four-month-old C57Bl/6 WT mice were injected into the tail vein with NEU1-GFP AV (n = 8) or GFP control AV (n = 8) at 10^9 pi/mouse, exposed to HFD and sacrificed after 20 weeks. (**A**) Relative mRNA expression levels of *Tnfα*, *Il6* and *Il1β* in liver and fat tissue samples determined by qRT-PCR (n = 6 for each group). (**B**) NEU1 activity was measured in liver homogenates at 8 (n = 2 for each group) and 20 weeks (n = 6 for each group) after AV injection using the fluorescent sialidase substrate 2'-(4-methylumbelliferyl)-α-D-*N*-acetylneuraminic acid. (**C**) Plasma total cholesterol (Chol), HDL, VLDL/LDL and triglycerides (TG) levels in mouse plasma (n = 6 for each group). (**D**) Liver mass values (normalized on body mass values) were similar between NEU1-GFP AV or GFP AV-infected mice (n = 6 for each group). Data are shown as means ± s.e.m. Significant (*$P < 0.05$, **$P < 0.01$, ***$P < 0.001$) difference was detected with GFP-AV group in *t*-test.

4. DISCUSSION

Multiple studies have established that sialylation and desialylation constitutes a novel type of modulation of activity of cellular receptors including IR (reviewed in [19]). Cells from sialidosis patients with genetic deficiency of NEU1 show impairment of insulin-induced phosphorylation of downstream protein kinase AKT, whereas treatment of these cells with purified NEU1 restores signaling, thus establishing a link between IR activation and NEU1 activity [16]. Moreover, mice with low NEU1 tissue levels demonstrated accelerated development of insulin resistance and diabetes in response to HFD and showed impaired insulin signaling in their muscle and liver tissues suggesting that the NEU1-dependent IR activation constitutes physiologically important pathway for regulation of glucose homeostasis [16]. At a molecular level, insulin binding to IR rapidly induces its interaction with NEU1, which hydrolyzes sialic acids in the glycan chains of the receptor and, consequently, induces its activation. The results obtained in the current study reveal the molecular mechanism of the IR activation by NEU1. We show that desialylation of IR by NEU1 induces a conformational change that increases interaction between the receptor subunits in the dimer (as revealed by the increase of BRET signal) and as previously established causes activation associated with signal transmission [40]. The inhibitor of NEU1, DANA blocks both interaction between the subunits and activation of the receptor. This proposed mechanism by which NEU1 activates the IR is consistent with previous report by Leconte et al. demonstrating that oligosaccharide side chains of the IR β-subunit are involved in the process of IR activation [41]. This study provided the first evidence that mutations of the N-glycosylation sites of the IR β-subunit alter the conformational changes of the receptor induced by insulin and dramatically impair its tyrosine kinase activity and autophosphorylation. Consequently the mutant receptor was unable to transduce important metabolic effects of insulin including glycogen synthesis and glucose transport [41].

Since the effect of supraphysiological levels of NEU1 on activation of IR was strong enough to restore insulin sensitivity in HepG2 cells treated in culture with palmitate, we explored if NEU1 can be used *in vivo* as a therapeutic target for insulin resistance. We treated obese C57Bl6 mice with glycemia and reduced insulin sensitivity with Ambroxol, which previously has been shown to increase NEU1 expression >3-fold [36]. This induced NEU1 expression and activity and reduced IR sialylation in mouse tissues, normalized the elevated fasting glucose levels and improved physiological and molecular response of mice to glucose and insulin injections. Importantly, the same treatment did not improve glucose tolerance or insulin sensitivity in obese NEU1-deficient $CathA^{S190A\text{-}Neo}$ mice, strongly suggesting that the effect of Ambroxol was mediated through NEU1 induction.

Encouraged by these results, we further tested if the long-term increase of NEU1 activity in one of the insulin target organs, liver though AV-mediated gene-transfer would protect mice from obesity-induced insulin resistance. To our surprise glycemia in NEU1-GFP AV-treated mice with 3–5-fold induced NEU1 activity levels in the liver tissue was higher than in mice treated with the control GFP virus, while the increase of the body mass was similar between the groups. In order to explain these results, we further tested whether NEU1-GFP AV-treated mice had distinct lipid blood profiles or higher fat liver content that could result in increased lipotoxicity, but could not find any difference with the control group in any of these parameters. It was also conceivable that NEU1-GFP AV-treated mice could have higher tissue inflammation level as a consequence of immune reaction to expressed human NEU1/CathA and/or viral capsid proteins. Still, the expression levels of inflammation markers, TNFα, IL-1-β and IL-6 in the liver and white adipose tissue of NEU1-GFP AV-infected mice were similar or lower than those in the control GFP AV-infected animals.

We suggest that the difference between the effects of Amboxol and NEU1-AV on insulin resistance might be partially explained by difference in the targeted tissue: skeletal muscle versus liver and/or the longevity of NEU1 overexpression: acute after Ambroxol versus chronic with AV. It is tempting to speculate that sustained supraphyisiological levels of NEU1 activity in liver may lead to the aberrant desialylation and constitutive activation of IR. In this case the long-term reduction of the IR expression could occur as a cellular response aimed on balancing this effect. This hypothesis is supported by lower levels of IR in liver tissues from NEU1-GFP AV-infected as compared with GFP AV-infected mice.

Interestingly, opposite effects of NEU1 on insulin signaling have been recently reported in literature. Blaise and co-workers have described that interaction between NEU1 and IR under chronic exposure to elastin-derived peptides reduces IR signaling [17]. Natori Y et al. showed that NEU1 activity is lower in liver and higher in epididymal fat of obese compared to non-obese mice and suggested that fluctuations in NEU1 activity might be associated with the pathological status of the tissues in obesity [15]. Similar discrepancy has been previously reported for the second plasma membrane neuraminidase, NEU3 that has also been shown to modulate insulin signaling, presumably by changing composition of membrane gangliosides [42,43]. Moreover, NEU3 protein abundance in the liver and skeletal muscle has been positively associated with tissue insulin sensitivity in the obesity and age-related rodent models of insulin resistance [44]. In line with these findings, Yoshizumi and colleagues demonstrated that AV-mediated hepatic NEU3 overexpression rapidly (1 week after infection) improved insulin sensitivity and glucose tolerance in mice fed HFD [42]. However, transgenic mice overexpressing the human NEU3 (with the highest activity increase observed in the muscle tissue) developed diabetic phenotype by 18–22 weeks associated with hyperinsulinemia, islet hyperplasia, and increased beta-cell mass [43]. Our previous work have shown that the levels of *Neu1* mRNA were increased in brain tissues of *Neu3* and *Neu4*-knockout mice suggesting the existence of mechanisms for compensatory regulation between the neuraminidase genes [45]. Although not tested here, it is possible that NEU3 expression in the NEU1-GFP AV-treated mice is decreased to compensate increased NEU1, which can partially contribute to the increased insulin resistance. Further studies are thus necessary to clarify the mechanism underlying the accelerated insulin resistance in response to AV-mediated NEU1 gene transfer. Nevertheless, it is apparent that sustained neuraminidase overexpression may lead to impaired insulin signaling in mice.

The current report for the first time demonstrates that acute pharmacological activation of NEU1 by Ambroxol reverses insulin resistance and glycemia in the mouse model, suggesting that NEU1 can be exploited as a pharmacological target for T2DM. Ambroxol is clinically used since 1978 as an expectorant and ingredient of anti-coughing syrups, tablets, and pastilles, but in the last decade the drug also attracted attention as a pharmacological non-active site chaperone for lysosomal β-glucocerebrosidase (GBA) mutant in a lysosomal Gaucher disease [46–48]. Since GBA mutations are associated with the development of Parkinson disease presumably through α-synuclein accumulation, multiple studies explored whether Ambroxol treatment also reduces α-synuclein levels (reviewed in [49]). Most recently, oral Ambroxol was demonstrated to cross the blood–brain barrier, and increase GBA activity in nonhuman primates as well as reduce brain α-synuclein levels in mice [50,51]. Ambroxol was thought to facilitate the correct folding of the mutant GBA in the ER and its transport to the lysosome, but later it has been demonstrated that Ambroxol also acts as an activator of the CLEAR network that includes ~100 genes encoding lysosomal proteins and proteins involved in lysosomal biogenesis [36]. These genes are under control of the transcription factor EB (TFEB) acting as a master regulator for the synchronized induction of the lysosomal network. NEU1 is among the genes activated by Ambroxol that provides an attractive opportunity for pharmacological induction of the NEU1 activity to restore insulin sensitivity. At the same time because of the wide spectrum of the Ambroxol targets, further studies are necessary to determine the longevity of the Ambroxol effect on the insulin sensitivity, potential side effects as well as the optimal dosage and the method of delivery of the drug required for effective treatment.

AUTHOR CONTRIBUTIONS

AF, XP and VS conducted experiments and analyzed the data. AF, XP, AVP, PT, and NH, designed experiments and analyzed the data. TI, BL, CWC and JAM provided essential materials for the study and analyzed the data. All authors participated in writing of the manuscript and approved it as submitted. Authors do not have conflict of interests regarding this manuscript.

ACKNOWLEDGMENTS

We thank Ms. Carla Martins for the help with testing the effect of Ambroxol on neuraminidase activity in cultured human fibroblasts and Dr. Mila Ashmarina for critically reading the manuscript. This work was partially supported by the research grants from Canadian Diabetes Association, Canadian Glycomics Network (C-2) and the Canadian Institutes of Health Research (111068) to AVP. AF was supported by FRSQ and Sainte-Justine UHC Foundation fellowships. AVP is a guarantor of this study and takes a full responsibility for its integrity.

CONFLICT OF INTEREST

None declared.

APPENDIX A. SUPPLEMENTARY DATA

Supplementary data related to this article can be found at https://doi.org/10.1016/j.molmet.2018.03.017.

REFERENCES

[1] Wild, S., Roglic, G., Green, A., Sicree, R., King, H., 2004. Global prevalence of diabetes: estimates for the year 2000 and projections for 2030. Diabetes Care 27:1047–1053.

[2] Chatterjee, S., Khunti, K., Davies, M.J., 2017. Type 2 diabetes. Lancet 389: 2239–2251.

[3] Saltiel, A.R., 2001. New perspectives into the molecular pathogenesis and treatment of type 2 diabetes. Cell 104:517–529.

[4] Saini, V., 2010. Molecular mechanisms of insulin resistance in type 2 diabetes mellitus. World Journal of Diabetes 1:68–75.

[5] Sparrow, L.G., Gorman, J.J., Strike, P.M., Robinson, C.P., McKern, N.M., Epa, V.C., et al., 2007. The location and characterisation of the O-linked glycans of the human insulin receptor. Proteins 66:261–265.

[6] Sparrow, L.G., Lawrence, M.C., Gorman, J.J., Strike, P.M., Robinson, C.P., McKern, N.M., et al., 2008. N-linked glycans of the human insulin receptor and their distribution over the crystal structure. Proteins 71:426–439.

[7] Hwang, J.B., Hernandez, J., Leduc, R., Frost, S.C., 2000. Alternative glycosylation of the insulin receptor prevents oligomerization and acquisition of insulin-dependent tyrosine kinase activity. Biochimica et Biophysica Acta 1499:74–84.

[8] Elleman, T.C., Frenkel, M.J., Hoyne, P.A., McKern, N.M., Cosgrove, L., Hewish, D.R., et al., 2000. Mutational analysis of the N-linked glycosylation sites of the human insulin receptor. Biochemical Journal 347(3):771–779.

[9] Yang, A., Gyulay, G., Mitchell, M., White, E., Trigatti, B.L., Igdoura, S.A., 2012. Hypomorphic sialidase expression decreases serum cholesterol by down-regulation of VLDL production in mice. The Journal of Lipid Research 53: 2573–2585.

[10] Fujioka, Y., Taniguchi, T., Ishikawa, Y., Yokoyama, M., 2000. Significance of acidic sugar chains of apolipoprotein B-100 in cellular metabolism of low-density lipoproteins. The Journal of Laboratory and Clinical Medicine 136: 355–362.

[11] Bartlett, A.L., Grewal, T., De Angelis, E., Myers, S., Stanley, K.K., 2000. Role of the macrophage galactose lectin in the uptake of desialylated LDL. Atherosclerosis 153:219–230.

[12] Suer Gokmen, S., Kazezoglu, C., Sunar, B., Ozcelik, F., Gungor, O., Yorulmaz, F., et al., 2006. Relationship between serum sialic acids, sialic acid-rich inflammation-sensitive proteins and cell damage in patients with acute myocardial infarction. Clinical Chemistry and Laboratory Medicine 44:199–206.

[13] Haq, M., Haq, S., Tutt, P., Crook, M., 1993. Serum total sialic acid and lipid-associated sialic acid in normal individuals and patients with myocardial infarction, and their relationship to acute phase proteins. Annals of Clinical Biochemistry 30(Pt 4):383–386.

[14] Gayral, S., Garnotel, R., Castaing-Berthou, A., Blaise, S., Fougerat, A., Berge, E., et al., 2014. Elastin-derived peptides potentiate atherosclerosis through the immune Neu1-PI3Kgamma pathway. Cardiovascular Research 102:118–127.

[15] Natori, Y., Ohkura, N., Nasui, M., Atsumi, G., Kihara-Negishi, F., 2013. Acidic sialidase activity is aberrant in obese and diabetic mice. Biological and Pharmaceutical Bulletin 36:1027–1031.

[16] Dridi, L., Seyrantepe, V., Fougerat, A., Pan, X., Bonneil, E., Thibault, P., et al., 2013. Positive regulation of insulin signaling by neuraminidase 1. Diabetes 62: 2338–2346.

[17] Blaise, S., Romier, B., Kawecki, C., Ghirardi, M., Rabenoelina, F., Baud, S., et al., 2013. Elastin-derived peptides are new regulators of insulin resistance development in mice. Diabetes 62:3807–3816.

[18] Monti, E., Miyagi, T., 2015. Structure and function of mammalian sialidases. Topics in Current Chemistry 366:183–208.

[19] Pshezhetsky, A.V., Hinek, A., 2011. Where catabolism meets signalling: neuraminidase 1 as a modulator of cell receptors. Glycoconjugate Journal 28: 441–452.

[20] Pshezhetsky, A.V., 2015. Crosstalk between 2 organelles: lysosomal storage of heparan sulfate causes mitochondrial defects and neuronal death in mucopolysaccharidosis III type C. Rare Diseases 3 e1049793.

[21] Arabkhari, M., Bunda, S., Wang, Y., Wang, A., Pshezhetsky, A.V., Hinek, A., 2010. Desialylation of insulin receptors and IGF-1 receptors by neuraminidase-1 controls the net proliferative response of L6 myoblasts to insulin. Glycobiology 20:603–616.

[22] Alghamdi, F., Guo, M., Abdulkhalek, S., Crawford, N., Amith, S.R., Szewczuk, M.R., 2014. A novel insulin receptor-signaling platform and its link to insulin resistance and type 2 diabetes. Cellular Signalling 26:1355–1368.

[23] Labbe, A., Nelles, M., Walia, J., Jia, L., Furlonger, C., Nonaka, T., et al., 2009. IL-12 immunotherapy of murine leukaemia: comparison of systemic versus gene modified cell therapy. Journal of Cellular and Molecular Medicine 13: 1962–1976.

[24] Luo, J., Deng, Z.L., Luo, X., Tang, N., Song, W.X., Chen, J., et al., 2007. A protocol for rapid generation of recombinant adenoviruses using the AdEasy system. Nature Protocols 2:1236–1247.

[25] Yoshimitsu, M., Sato, T., Tao, K., Walia, J.S., Rasaiah, V.I., Sleep, G.T., et al., 2004. Bioluminescent imaging of a marking transgene and correction of Fabry mice by neonatal injection of recombinant lentiviral vectors. Proceedings of the National Academy of Sciences of the United States of America 101:16909–16914.

[26] Issad, T., Boute, N., Pernet, K., 2002. A homogenous assay to monitor the activity of the insulin receptor using Bioluminescence Resonance Energy Transfer. Biochemical Pharmacology 64:813–817.

[27] Boute, N., Pernet, K., Issad, T., 2001. Monitoring the activation state of the insulin receptor using bioluminescence resonance energy transfer. Molecular Pharmacology 60:640–645.

[28] Guo, T., Datwyler, P., Demina, E., Richards, M.R., Ge, P., Zou, C., et al., 2018. Selective inhibitors of human neuraminidase 3. Journal of Medicinal Chemistry 61:1990–2008.

[29] Cousin, S.P., Hugl, S.R., Wrede, C.E., Kajio, H., Myers Jr., M.G., Rhodes, C.J., 2001. Free fatty acid-induced inhibition of glucose and insulin-like growth factor I-induced deoxyribonucleic acid synthesis in the pancreatic beta-cell line INS-1. Endocrinology 142:229–240.

[30] Issad, T., Combettes, M., Ferre, P., 1995. Isoproterenol inhibits insulin-stimulated tyrosine phosphorylation of the insulin receptor without increasing its serine/threonine phosphorylation. European Journal of Biochemistry 234:108–115.

[31] Seyrantepe, V., Hinek, A., Peng, J., Fedjaev, M., Ernest, S., Kadota, Y., et al., 2008. Enzymatic activity of lysosomal carboxypeptidase (cathepsin) A is required for proper elastic fiber formation and inactivation of endothelin-1. Circulation 117:1973–1981.

[32] Martins, C., Hulkova, H., Dridi, L., Dormoy-Raclet, V., Grigoryeva, L., Choi, Y., et al., 2015. Neuroinflammation, mitochondrial defects and neurodegeneration in mucopolysaccharidosis III type C mouse model. Brain 138:336–355.

[33] Allain, C.C., Poon, L.S., Chan, C.S., Richmond, W., Fu, P.C., 1974. Enzymatic determination of total serum cholesterol. Clinical Chemistry 20:470–475.

[34] Roeschlau, P., Bernt, E., Gruber, W., 1974. Enzymatic determination of total cholesterol in serum. Zeitschrift für Klinische Chemie und Klinische Biochemie 12:226.

[35] Dong, X., Bi, L., He, S., Meng, G., Wei, B., Jia, S., et al., 2014. FFAs-ROS-ERK/P38 pathway plays a key role in adipocyte lipotoxicity on osteoblasts in co-culture. Biochimie 101:123—131.

[36] McNeill, A., Magalhaes, J., Shen, C., Chau, K.Y., Hughes, D., Mehta, A., et al., 2014. Ambroxol improves lysosomal biochemistry in glucocerebrosidase mutation-linked Parkinson disease cells. Brain 137:1481—1495.

[37] Pacienza, N., Yoshimitsu, M., Mizue, N., Au, B.C., Wang, J.C., Fan, X., et al., 2012. Lentivector transduction improves outcomes over transplantation of human HSCs alone in NOD/SCID/Fabry mice. Molecular Therapy 20:1454—1461.

[38] Langford-Smith, K.J., Mercer, J., Petty, J., Tylee, K., Church, H., Roberts, J., et al., 2011. Heparin cofactor II-thrombin complex and dermatan sulphate: chondroitin sulphate ratio are biomarkers of short- and long-term treatment effects in mucopolysaccharide diseases. Journal of Inherited Metabolic Disease 34:499—508.

[39] Desai, U.J., Slosberg, E.D., Boettcher, B.R., Caplan, S.L., Fanelli, B., Stephan, Z., et al., 2001. Phenotypic correction of diabetic mice by adenovirus-mediated glucokinase expression. Diabetes 50:2287—2295.

[40] Hubbard, S.R., 1997. Crystal structure of the activated insulin receptor tyrosine kinase in complex with peptide substrate and ATP analog. The EMBO Journal 16:5572—5581.

[41] Leconte, I., Auzan, C., Debant, A., Rossi, B., Clauser, E., 1992. N-linked oligosaccharide chains of the insulin receptor beta subunit are essential for transmembrane signaling. Journal of Biological Chemistry 267:17415—17423.

[42] Yoshizumi, S., Suzuki, S., Hirai, M., Hinokio, Y., Yamada, T., Yamada, T., et al., 2007. Increased hepatic expression of ganglioside-specific sialidase, NEU3, improves insulin sensitivity and glucose tolerance in mice. Metabolism 56:420—429.

[43] Sasaki, A., Hata, K., Suzuki, S., Sawada, M., Wada, T., Yamaguchi, K., et al., 2003. Overexpression of plasma membrane-associated sialidase attenuates insulin signaling in transgenic mice. Journal of Biological Chemistry 278:27896—27902.

[44] Lipina, C., Nardi, F., Grace, H., Hundal, H.S., 2015. NEU3 sialidase as a marker of insulin sensitivity: regulation by fatty acids. Cellular Signalling 27:1742—1750.

[45] Pan, X., De Aragao, C.B.P., Velasco-Martin, J.P., Priestman, D.A., Wu, H.Y., Takahashi, K., et al., 2017. Neuraminidases 3 and 4 regulate neuronal function by catabolizing brain gangliosides. The FASEB Journal 31:3467—3483.

[46] Maegawa, G.H., Tropak, M.B., Buttner, J.D., Rigat, B.A., Fuller, M., Pandit, D., et al., 2009. Identification and characterization of ambroxol as an enzyme enhancement agent for Gaucher disease. Journal of Biological Chemistry 284:23502—23516.

[47] Zimran, A., Altarescu, G., Elstein, D., 2013. Pilot study using ambroxol as a pharmacological chaperone in type 1 Gaucher disease. Blood Cells Molecules and Diseases 50:134—137.

[48] Bendikov-Bar, I., Maor, G., Filocamo, M., Horowitz, M., 2013. Ambroxol as a pharmacological chaperone for mutant glucocerebrosidase. Blood Cells Molecules and Diseases 50:141—145.

[49] O'Regan, G., deSouza, R.M., Balestrino, R., Schapira, A.H., 2017. Glucocerebrosidase mutations in Parkinson disease. Journal of Parkinson's Disease.

[50] Migdalska-Richards, A., Daly, L., Bezard, E., Schapira, A.H., 2016. Ambroxol effects in glucocerebrosidase and alpha-synuclein transgenic mice. Annals of Neurology 80:766—775.

[51] Migdalska-Richards, A., Ko, W.K.D., Li, Q., Bezard, E., Schapira, A.H.V., 2017. Oral ambroxol increases brain glucocerebrosidase activity in a nonhuman primate. Synapse, 71.

